VECTOR CONTROL OF A POSITION SENSORLESS SPMSM DRIVE WITH RNN BASED STATOR FLUX ESTIMATOR

Kalyan Kumar HALDER Md. HABIBULLAH Naruttam Kumar ROY Md. Abdur RAFIQ
Dept. of EEE, Khulna University of Engineering & Technology, Khulna-9203, Bangladesh,
Email: kalyan_kuet@yahoo.com, mhueeekuet@gmail.com, nkroy@yahoo.com, mdabdurrafiq2003@yahoo.com

B. C. GHOSH
Dept. of EEE, American International University-Bangladesh, Dhaka-1213, Bangladesh,
Email: bcgkuet@aiub.edu

Abstract: *A position sensorless Surface Permanent Magnet Synchronous Motor (SPMSM) drive based on single layer Recurrent Neural Network (RNN) is presented in this paper. The motor equations are written in rotor fixed d-q reference frame. A PID controller is used to process the speed error to generate the reference torque current keeping the magnetizing current fixed. The RNN estimator is used to estimate flux components along the stator fixed stationary axes (α-β). The flux angle and the reference current phasor angle are used in vector rotator to generate the reference phase currents. Hysteresis current controller block controls the switching of the three phase inverter to apply voltage to the motor stator. Simulation studies on different operating conditions indicate the acceptability of the drive system. The proposed estimator can be used to accurately measure the motor fluxes and rotor angle over a wide speed range. The proposed control scheme is robust under load torque disturbances and motor parameter variations. It is also simple and low cost to implement in a practical environment.*

Key words: *Surface permanent magnet synchronous motor, robust control, sensorless control, recurrent neural network, and hysteresis current controller.*

1. Introduction

In recent years, permanent magnet synchronous motor (PMSM) drives have been widely used in many industrial applications such as robots, rolling mills, machine tools, etc. The inherent advantages of these machines include high power density, low inertia, and high speed capabilities. However, the control performance of the PMSM is greatly affected by the uncertainties of the plant which are usually mismatched motor parameters, external load disturbances, unmodelled and non-linear dynamics [1]. Hence, different control schemes are adopted for speed controlling purposes. Study of PMSM drives are a topic of interest of current researchers. A permanent magnet synchronous motor has permanent magnets to produce the air gap magnetic field. PM machines are generally classified as [2]: (1) the popularly used surface permanent magnet (SPM) machines in which magnets are mounted on the rotor surface and (2) the buried or interior permanent magnet (IPM) machines in which magnets are mounted inside the rotor. SPM motors have q-axis inductance equal to the d-axis inductance. Torque angle control under constant torque operation (within base speed) and flux control as an additional component for higher speeds is proposed in [2].

Driving a PMSM requires the rotor position information to control the motor torque which is generally detected by mechanical position sensors such as an encoder or a resolver. Many papers about position sensorless drive of PMSM have been published, [3, 4] as for examples. Flux estimation can be applied to detect the rotor position and is considered as an important task in implementing high-performance motor drives [5]. The methodology of vector control is normally developed based on estimation of pole position of the SPMSM. The estimators are designed using current or voltage models of the motor. Integration or low pass filter-based flux estimators introduce error due to dc offset value. To solve the problem notch filter was introduced in [6]. The same methodology was applied through adaptive integration ANN estimators [7] for induction motors. In [8], a sensorless zero-sequence (SZS) air-gap flux estimation technique was proposed to realize field-oriented induction motor drives without speed and current sensors, able to operate down to zero speed. A flux estimator for induction motor was proposed in [9] and reported to be almost insensitive to parameter variations. Encoder-less operation of IPM motor was proposed in [10]. In this strategy, the observer used is a sliding mode type and the main control aspect is direct torque control. In [11], the authors proposed a motion-sensorless motor control of permanent magnet-assisted reluctance synchronous machine from zero speed up to maximum speed, using direct torque and flux control with space vector modulation. An improved method of estimating flux

A part of this paper was presented in the 6th International Conference on Electrical & Computer Engineering 2010 (ICECE 2010), Dhaka, Bangladesh, December 2010.

angle, rotor position, and velocity by tracking the position of spatial saliencies in an AC machine was proposed in [12].

SPMSM drives are generally of low power category and require simple and cost-effective controllers. This paper investigates a robust control of a position sensorless SPMSM drive. A mathematical model of SPMSM using the flux estimator is utilized to estimate the rotor position. A neural network based adaptive integration methodology is proposed for stator flux estimation to improve the transient and steady state performances. Estimated flux is obtained from speed error and current by an integrating method accomplished by Programmable Cascaded Low Pass Filter (PCLPF) implemented by neural network. The neural network consists of RNN and a Feed-Forward Artificial Neural Network (FFANN). Moreover, the hysteresis controller is used to control the current in such a way that it can follow the command current as close as possible to the sinusoidal reference. The performances of the proposed drive system have also been studied due to load torque change, parameter variations, and speed reversal.

2. Mathematical Model

The cross-sectional layout of a surface mounted permanent magnet motor is shown in Fig. 1. The stator has balanced three-phase windings, which produces a near sinusoidal distribution of mmf dependent on the value of the stator current. The magnets are mounted on the surface of the motor core. They have the same role as the field winding in a synchronous machine except that their magnetic field is constant and there is no control on it [13].

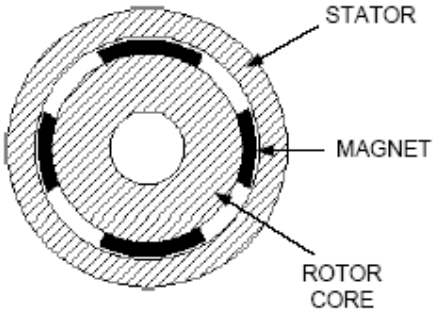

Fig. 1 Structure of the SPMSM

Conventionally a two phase lumped parameter equivalent circuit model in mutually perpendicular frame (d-q model) has been used to analyze reluctance synchronous machines [14]. This theory is now applied in analysis of other types of motors such as PM synchronous motors and induction motors. The SPMSM flux due to permanent magnet acts along d-axis. The stator voltages and currents act along the physical symmetric a-b-c-axes. The currents along these axes produce torque and also magnetizing current components, i_t and i_m respectively, in mutually perpendicular axes. The stationary axes a-, b-, c-, their two phase equivalents along α-, β-axes, and the rotating axes are shown in Fig 2. In this representation δ is the torque angle and ψ is the instantaneous angle of the reference north pole of SPMSM.

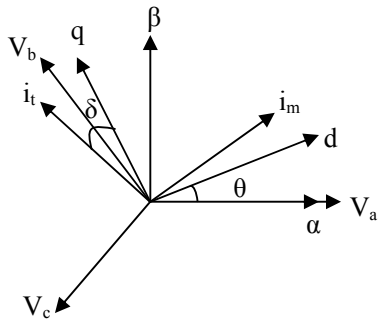

Fig. 2 Stationary and rotating axes of SPMSM

A mathematical model of the SPMSM is required for proper simulation of the system and to design a suitable controller.The dynamic model of the PMSM can be described in the d-q rotor frame as follows:

$$v_q = R_s i_q + p\lambda_q + \omega_e \lambda_d \quad (1)$$

$$v_d = R_s i_d + p\lambda_d - \omega_e \lambda_q \quad (2)$$

The flux linkages along the d-q axis are given by:

$$\lambda_q = L_q i_q \quad (3)$$

$$\lambda_d = L_d i_d + \psi_f \quad (4)$$

Where, v_d and v_q are the d-q axis voltages, i_d and i_q are the d-q axis stator currents, L_d and L_q are the d-q axis inductances, λ_d and λ_q are the d-q axis stator flux linkages respectively, R_s is the stator resistance per phase, ψ_f is the permanent magnetic flux, ω_e is the electrical angular velocity, and p is the derivative operator ($\equiv d/dt$).

The developed electromagnetic torque is given as:

$$T_e = \frac{3P_p}{2}(\psi_f i_q + (L_d - L_q) i_d i_q) \quad (5)$$

The torque balance equation for the motor speed dynamics is given by

$$T_e = T_L + J_m p\omega_m + B_m \omega_m \quad (6)$$

For simulation under transient conditions, the model equations of the PMSM must be expressed in state-space form as:

$$L_q \frac{di_q}{dt} = v_q - R_s i_q - P_p \omega_m L_d i_d - P_p \omega_m \psi_f \quad (7)$$

$$L_d \frac{di_d}{dt} = v_d - R_s i_d + P_p \omega_m L_q i_q \quad (8)$$

$$J_m \frac{d\omega_m}{dt} = T_e - T_L - B_m \omega_m \quad (9)$$

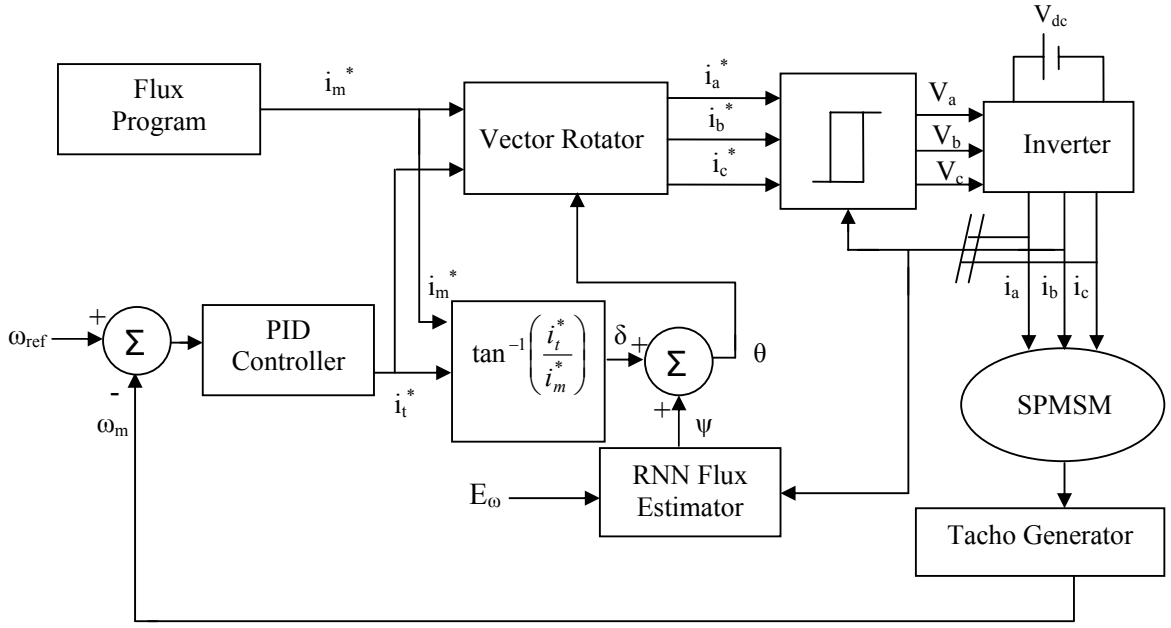

Fig. 3 Control Scheme of the SPMSM

and $\omega_e = p_p \cdot \omega_m$ (10)

Where, ω_m is the rotor mechanical speed and P_p is the number of pole pairs.

3. Proposed Control Scheme

The high performance control strategy is implemented in closed loop using PID controller. This requires speed error to be processed in closed loop to generate the torque producing component of the stator current (i_t^*). The total control scheme of the drive system is shown in Fig. 3. The selection of suitable values for gain constants was carried out for different combinations of K_p, K_i and K_d after having their initial guesses following the ideas in [15]. Finally, the following sets were arrived for the PID controller: $K_p = 6.0$, $K_i = 0.042$, and $K_d = 0.55$.

The components of current i_m^* and i_t^* are used to generate the three phase reference currents i_a^*, i_b^*, and i_c^*. These reference currents are then compared with the actual motor currents i_a, i_b, and i_c to generate PWM switching signals, which will turn on or turn off the power semiconductor devices of the three-phase inverter to produce the actual voltages to the motor.

The torque angle, $\delta = \tan^{-1}\left(\frac{i_t^*}{i_m^*}\right)$ (11)

The flux angle, $\psi = \tan^{-1}\left(\frac{\lambda_{\beta s}}{\lambda_{\alpha s}}\right)$ (12)

Estimated angle of current phasor with respect to reference pole, $\theta = \delta + \psi$ (13)

The reference currents to be adjusted are formulated as follows:

$$i_a^* = i_m^* \cos\theta - i_t^* \sin\theta \quad (14)$$

$$i_b^* = i_m^* \cos(\theta - 120^0) - i_t^* \sin(\theta - 120^0) \quad (15)$$

$$i_c^* = i_m^* \cos(\theta + 120^0) - i_t^* \sin(\theta + 120^0) \quad (16)$$

The stationary 3-axes (a-, b-, c-) to stationary 2-axes fictitious (α-, β-) transformation is given by

$$i_{\alpha s} = i_a - 0.5\, i_b - 0.5\, i_c \quad (17)$$

$$i_{\beta s} = \frac{\sqrt{3}}{2}(i_b - i_c) \quad (18)$$

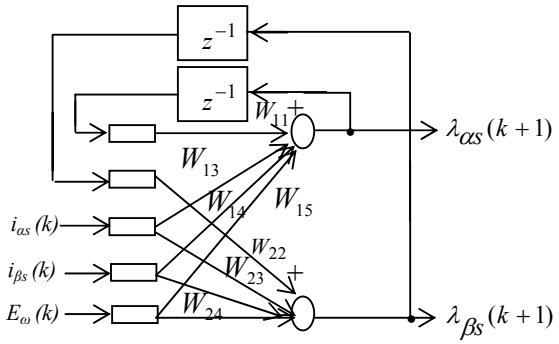

Fig. 4 Stationary α- and β-axis stator flux estimation by RNN

3.1 RNN Based Stator Flux Estimation

In the proposed algorithm stator flux is estimated from stationary α-β axes stator currents and speed error, E_ω. An equivalent RNN is then proposed which results in the following matrix equation:

$$\begin{bmatrix}\lambda_{\alpha s}(k+1)\\ \lambda_{\beta s}(k+1)\end{bmatrix}=\begin{bmatrix}W_{11} & 0\\ 0 & W_{22}\end{bmatrix}\begin{bmatrix}\lambda_{\alpha s}(k)\\ \lambda_{\beta s}(k)\end{bmatrix}$$
$$+\begin{bmatrix}W_{13}\\ W_{23}\end{bmatrix}i_{\alpha s}(k)+\begin{bmatrix}W_{14}\\ W_{24}\end{bmatrix}i_{\beta s}(k)+\begin{bmatrix}W_{15}\\ W_{25}\end{bmatrix}E_{\omega}(k) \qquad (19)$$

Where, W_{11}, W_{13}, W_{22}, W_{23}, W_{14} etc. are the weights of the RNN, which is shown in Fig. 4. The weights indicated by the different line segments are adjusted by training the neural network by a Real Time Recurrent Learning (RTRL) algorithm.

3.2 Hysteresis Current Control Scheme

The main task of the current controller is to force the current vector in the three phase load according to a reference trajectory. The block diagram of a three-phase hysteresis current controller is shown in Fig. 5. The power circuit of the drive system is shown in Fig. 6. The scheme compares the phase currents with the desired values within the hysteresis band to take decision on switching of inverter transistor. The switching logic is formulated as given below:

if $i_a < (i_a^* - hb)$ T1 on and T4 off;
if $i_a > (i_a^* + hb)$ T1 off and T4 on;
if $i_b < (i_b^* - hb)$ T3 on and T6 off;
if $i_b > (i_b^* + hb)$ T3 off and T6 on;
if $i_c < (i_c^* - hb)$ T5 on and T2 off;
if $i_c > (i_c^* + hb)$ T5 off and T2 on;

Where, hb is the hysteresis band around the reference currents.

4. Simulation Results

Simulation studies have been conducted in order to test the performance of the drive system. The system under consideration was simulated in a Pentium-based PC with C++ environment. The machine model is considered in d-q axes frame. Reference phase currents are generated from the required torque and magnetizing currents i_t^* and i_m^*. The phase voltages V_a, V_b, and V_c resulting from the hysteresis current controller are transformed into d- and q-axes quantities V_d and V_q. Currents obtained from simulation model are transferred to get the actual phase currents. The rating and motor parameters used in this simulation are given in Appendix. The incremental time Δt for simulating the system was 5 μs.

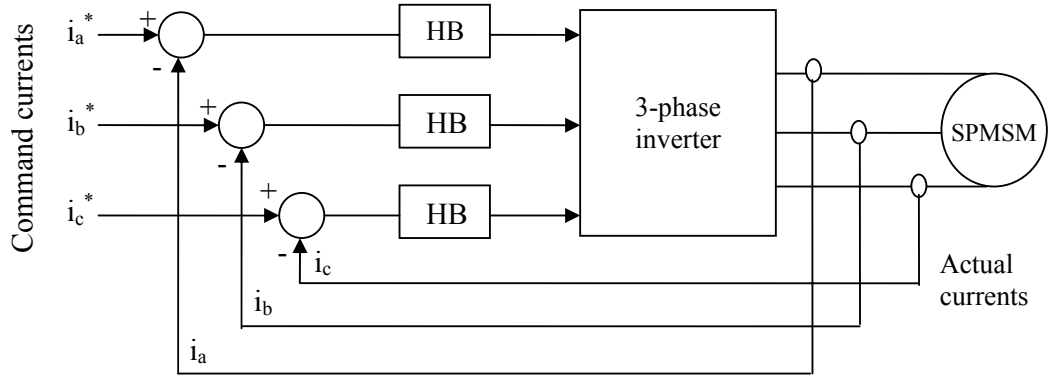

Fig. 5 Hysteresis-Band (HB) current controller block diagram

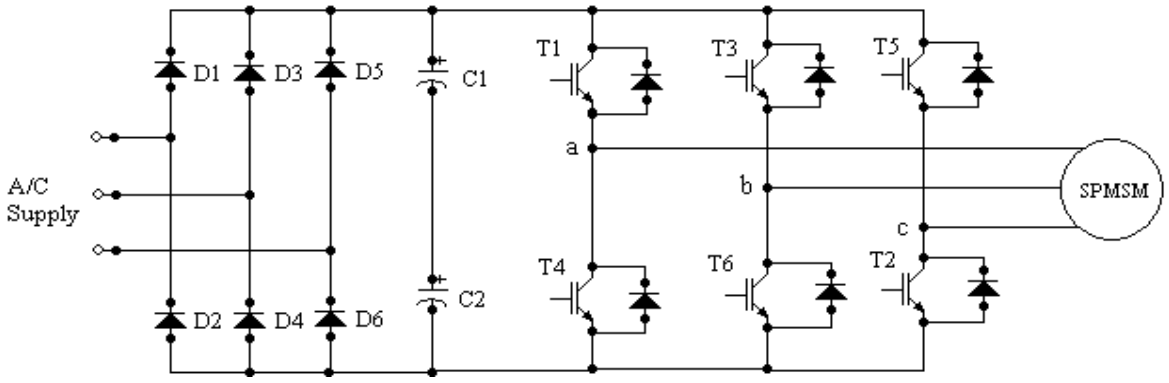

Fig. 6 Power circuit of the drive system

4.1 Performance of Flux and Angle Estimator

The effectiveness of the proposed flux estimator along α-β axes needs to be verified before implementing it in the drive system. Real time flux components calculated from exact values of motor variables are computed and compared with the estimated flux components. Fig. 7 gives a comparison between the actual and estimated values of α-β axes stator fluxes and rotor angle when the motor runs at 4500 rpm. A complete matching of the variables is indicated in the figures. Fig. 8 gives a comparison between the actual and estimated values of the stator fluxes and rotor angle when the motor runs at 45 rpm. The estimated and actual values are in good agreement. Clearly, the proposed RNN estimator can be used to accurately estimate fluxes and rotor angle at both high- and low-motor speeds.

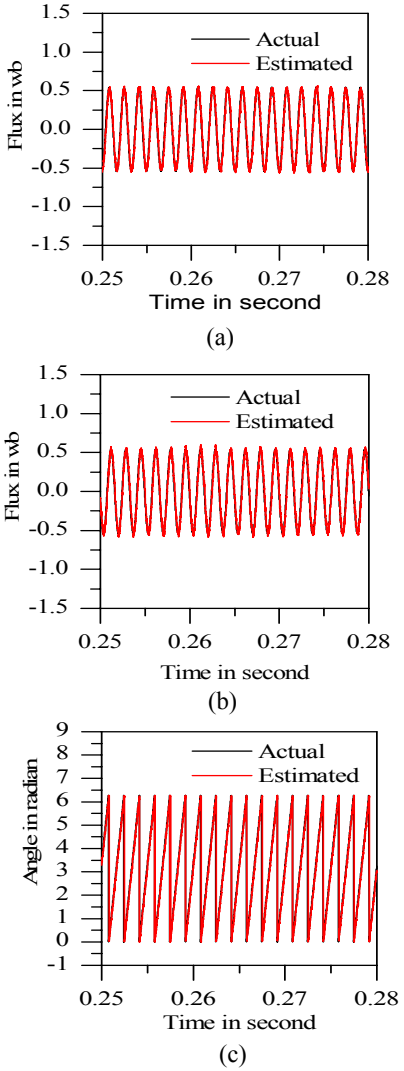

Fig. 7 Estimated and actual components of (a) α-axis flux, (b) β-axis flux, and (c) rotor angle for the SPMSM runs at 4500 rpm

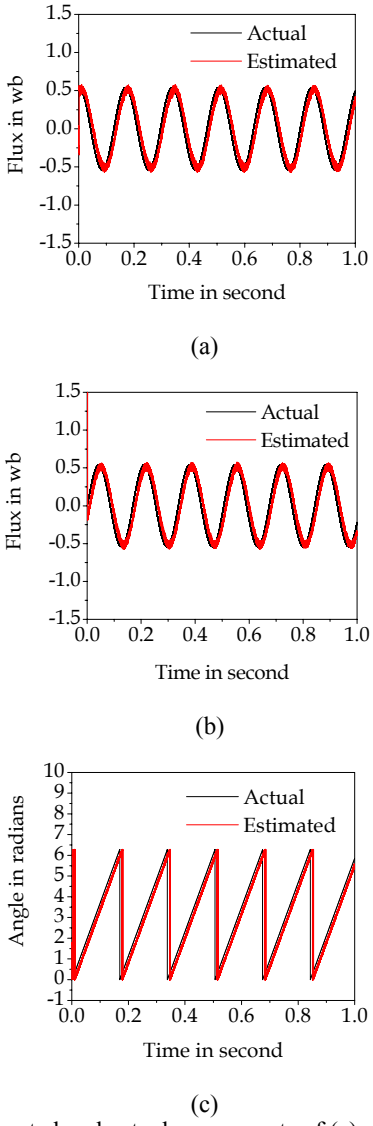

Fig. 8 Estimated and actual components of (a) α-axis flux, (b) β-axis flux, and (c) rotor angle for the SPMSM runs at 45 rpm

4.2 Starting Performance of the SPMSM Drive

The motor was started with a command speed of 4500 rpm from standstill condition. Fig. 9 (a) shows the simulated speed response of the drive at rated speed condition. It is seen that it follows the command speed as fast as possible at t=0.23 sec. Thus, the SPMSM drive shows better performances as very fast speed response with no overshoot. Fig. 9 (b) shows the developed torque that oscillates around the load torque when the set speed is reached. It is noticed that higher electromagnetic torque is generated during the motor acceleration. Some oscillations in electromagnetic torque is noticed which is due to switching of the devices with hysteresis controller. Figs. 9 (c) and (d) show the reference and actual phase

currents for the motor under transient and steady-state conditions. Very small switching notches are shown in actual current waveforms that do not affect the motor performance. The effectiveness of the hysteresis current controller is established from these figures.

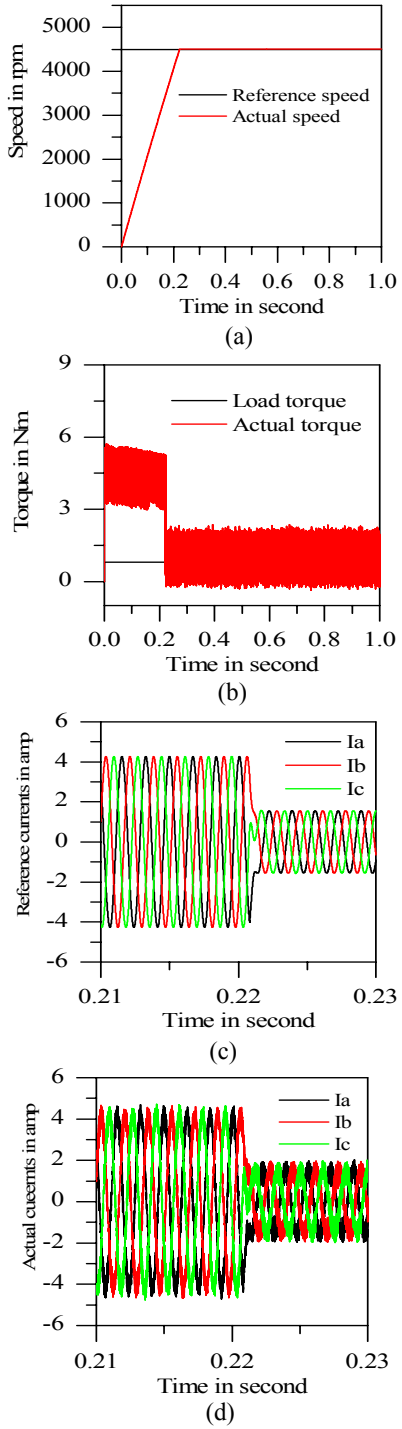

Fig. 9 (a) Simulated speed response, (b) Developed electromagnetic torque, (c) Three phase reference currents, and (d) Three phase actual currents for the SPMSM drive at starting condition

4.3 Performance under Different Operating Conditions

4.3.1 Sudden Change in Load Torque

Initially the motor starts from standstill with load torque 0.8 Nm. Suddenly at t=0.5 seconds load torque is increased to 1.4 Nm. The developed electromagnetic torque and speed response with change of load at t=0.5 seconds is given in Figs. 10 (a) and (b). Sudden application of load torque causes no oscillation in speed. The steady-state error is negligible. Figs. 10(c) and (d) show the actual phase currents and torque angle for change in load torque respectively.

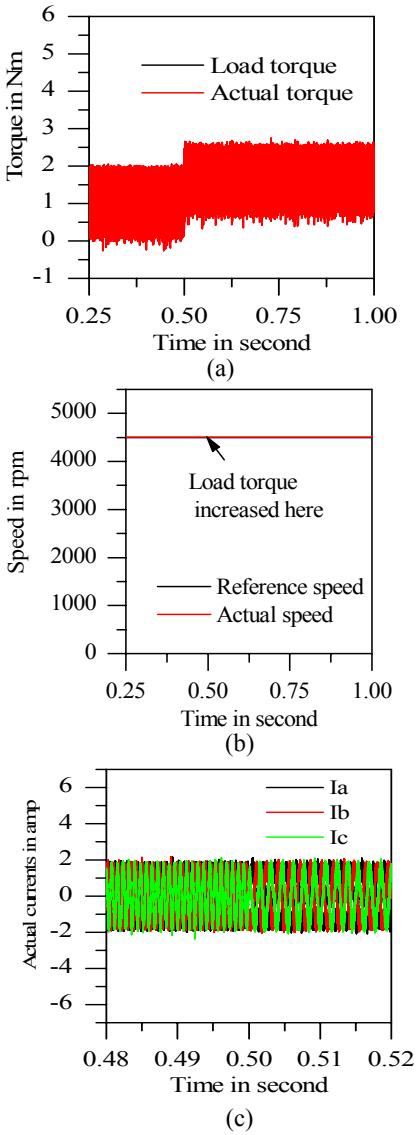

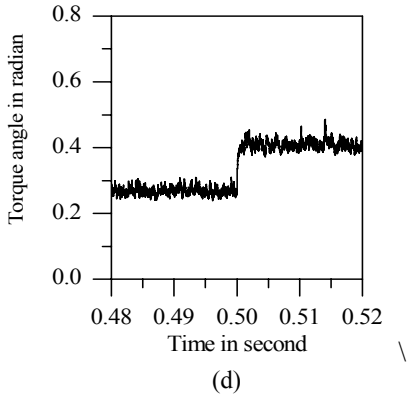

(d)

Fig. 10 (a) Developed electromagnetic torque**,** (b) Simulated speed response, (c) Actual phase currents and (d) Torque angle for the SPMSM drive for change in load torque (0.8 Nm to 1.4 Nm)

4.3.2 Variation of Stator Resistance

The stator resistance is increased to double at t=0.5 seconds. Fig. 11 (a) shows the effect of stator resistance on speed. The speed does not drop at all due to change of stator resistance. The change in resistance has negligible effect on accuracy of flux and rotor position estimation as shown in Fig. 11 (b). Thus drive performance is independent of stator resistance variation.

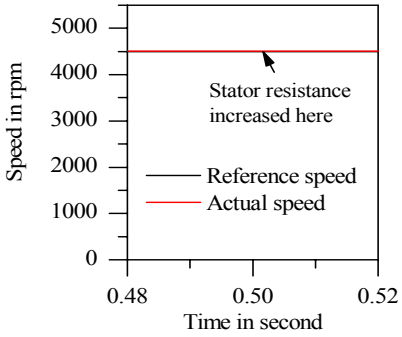

(a)

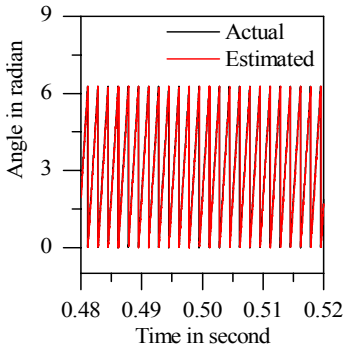

(b)

Fig. 11 (a) Simulated speed response, and (b) Estimated and actual rotor angle for change in stator resistance

4.3.3 Variation of Stator Inductances

The stator inductances (d-q axes) are increased to double at t=0.5 seconds. Fig. 12 (a) shows the effect of inductances on speed. The speed does not drop due to change of q-axis and d-axis inductances. Also it has almost no effect on the accuracy of flux and rotor position estimation as shown in Fig. 12 (b). Thus drive performance is insensitive of inductance variation.

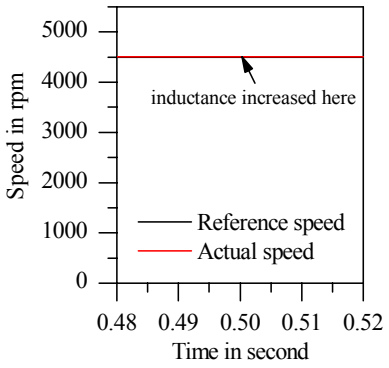

(a)

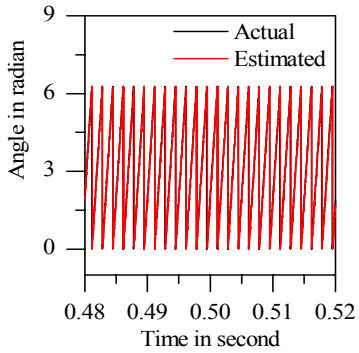

(b)

Fig. 12 (a) Simulated speed response, and (b) Estimated and actual rotor angle for change in stator inductances

4.3.4 Reversal of Speed

Fig. 13 (a) shows the speed response for different set of speed. It is observed that the drive system follows a linear pattern and takes a little bit higher time when the speed is reversed from +4500 rpm to -4500 rpm in comparison to starting condition (0 to +4500 rpm). But when it is reversed from -4500 rpm to +4500 rpm then it takes almost double time than the starting condition. Fig. 13 (b) shows corresponding developed electromagnetic torque.

5. Conclusions

The paper presents a robust control strategy with RNN flux estimator for a position sensorless SPMSM which is capable to produce very fast dynamic response. Simulation results show that the proposed

drive is able to deliver accurate estimation of flux and position both in steady-state and transient conditions. Simulation results show that the proposed control scheme is sufficiently stable and is robust to load disturbance, parameter variations, and speed reversal condition. Very fast response of the system without oscillation indicates the effectiveness of the proposed control scheme.

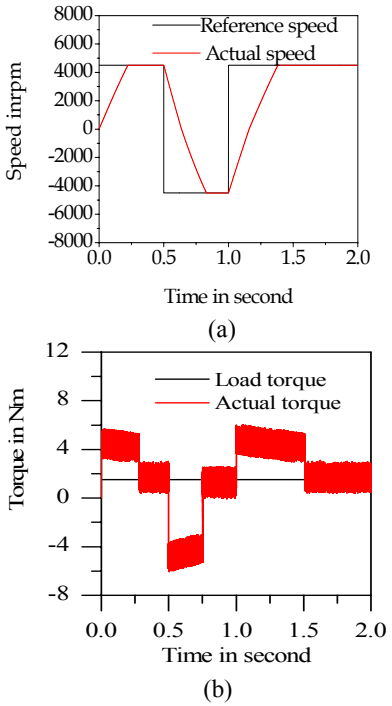

Fig. 13 (a) Simulated speed response and (b) Developed electromagnetic for change in reference speed

APPENDIX

The SPMSM parameters, RNN weights are given below:
Rating: 3-phase, 950W, 325V, 2.7A, 2-pole pair,
Parameters:
Stator resistance, R_s = 2.45 Ω
d-axis inductance, L_d = 4.25 mH
q-axis inductance, L_q = 4.25 mH
Motor inertia, J_m = 0.0016 Kg-m^2
Rated torque, T_b = 1.44 Nm
Friction coefficient, B_m = 0.0008 Nm/rad/sec
Magnetic flux constant, ψ_f (rms) = 0.533 Wb
Weights of the RNN: $W_{11} = W_{22} = 0.945$, $W_{13} = W_{23} = 0.01$, $W_{14} = 0.008$, $W_{24} = -0.008$, $W_{15} = W_{25} = 0.0001$

References

1. Lin, F.-J.: *A Real Time Position Controller Design with Torque Feedforward Control for PM Synchronous Motor*. In: IEEE Trans. on Industrial Electronics, Vol. 44, No. 3, pp. 398-407, June 1997,USA.
2. Bose, B. K.: *A High-Performance Inverter-Fed Drive System of an Interior Permanent Magnet Synchronous Machine*. In: IEEE Trans. on Industry Appli., Vol. 24, No. 6, pp. 987-997, Nov. /Dec. 1988, USA.
3. Tanaka, K., Miki, I.: *Position Sensorless Control of Interior Permanent Magnet Synchronous Motor Using Extended Electromotive Force*. In: Electrical Engineering in Japan, Vol. 161, No. 3, pp. 41-48, 2007, Japan.
4. Chen, Z., Tomito, M., Doki, S., Okuma, S.: *An Extended Electromotive Force Model for Sensoless Control of Interior Permanent Magnet Synchronous Motor Drive*. In: IEEE Trans. on Industrial Electronics, Vol. 50, No. 2, pp. 288-295, April 2003, USA.
5. Wu, R., Slemon, G. R.: *A Permanent Magnet Motor Drive without a Shaft Sensor*. In: IEEE Trans. Ind. Appli., Vol. 27, No. 5, pp. 1005–1011, 1991, USA.
6. Jun, H., Wu, B.: *New Integration Algorithms for Estimating Motor Flux over a Wide Speed Range*. In: IEEE Trans. on Power Electronics, Vol. 13, No. 5, pp. 969-977, September 1998, USA.
7. Cirrincione, M., Pucci, M., Cirrincione, G., and Capolino, G.: *A New Adaptive Integration Methodology for Estimating Flux in Induction Machine Drives*. In: IEEE Trans. on Power Electronics, Vol. 19, No. 1, pp. 25-33, January 2004, USA.
8. Consoli, A., Scarcella, G., Testa, A.: *Speed- and current-sensorless field-oriented induction motor drive operating at low stator frequencies*. In: IEEE Trans. on Industry Appli., Vol. 40, No. 1, pp. 186 - 193, Jan/Feb 2004, USA.
9. Abdur Rafiq, M., Golam Sarwer, M., Ghosh, B.C.*: Fast Speed Response Field-Orientation Control of Induction Motor Drive with Adaptive Neural Integrator*. In: Istanbul University-Journal of Electrical & Electronics Engineering, Vol. 6, No. 2, pp. 229-235, 2006, Turkey.
10. Xu Z., Rahman M. F.: *Encoder-Less Operation of a Direct Torque Controlled IPM Motor Drive with a Novel Sliding Mode Observer*. In: Proceedings of the AUPEC 2004, September 26-29, 2004, Brisbane, Australia.
11. Boldea, I., Pitic, C. I., Lascu, C., Andreescu G.-D., Tutelea, L., Blaabjerg, F., Sandholdt, P.: *DTFC-SVM Motion-Sensorless Control of a PM-Assisted Reluctance Synchronous Machine as Starter-Alternator for Hybrid Electric Vehicles*. In: IEEE Trans. on Power Electronics, Vol. 21, No. 3, pp. 711-719, May 2006, USA.
12. Degner, M.W., Lorenz, R. D.: *Using multiple saliencies for the estimation of flux, position, and velocity in AC machines*. In: IEEE Trans. on Industry Appli., Vol. 34, No. 5, pp. 1097 - 1104, Sep/Oct 1998, USA.
13. Sebastian, T., Slemon, G. R.: *Transient Modeling and Performance of Variable Speed Permanent Magnet Motors*. In: IEEE Trans. on Industry Appli., Vol. 25, No. 1, pp. 101-106, Sep. 1986, USA.
14. Krause, P.C.: *Analysis of Electric Machinery*, McGraw-Hill, 1986.
15. Bologani, S., Buja, G. S.: *Control System Design of a Current Inverter Induction Motor Drives*. In: IEEE Trans. on Industry Appli., Vol. IA-21, No. 5, pp. 1145-1153, Sep. 1985, USA.